Millimeter Thin and Rubber-Like Solid-State Lighting Modules Fabricated Using Roll-to-Roll Fluidic Self-Assembly and Lamination

*Se-Chul Park, Shantonu Biswas, Jun Fang, Mahsa Mozafari, Thomas Stauden, and Heiko O. Jacobs**

The field of stretchable electronics has seen a rapid increase in research activities in recent years. It enables new kinds of applications such as smart clothing,[1] conformable photovoltaics,[2] stretchable batteries,[3,4] artificial electronic skins,[5,6] or mechanically soft and conformable health monitoring devices[7,8] to give a few recent examples. The realization typically requires integration of functional semiconductor materials on a low-temperature stretchable polymeric rubber-like support that is in stark contrast to traditional semiconductor manufacturing which requires the use of high-temperature processing and rigid semiconductor wafers. From a technical point of view, a classification into two groups can be made: Class 1 – "polymeric substrate first" uses the low-temperature polymeric substrates right at the outset of the processing sequence. Commonly direct-write techniques are subsequently used to deposit the required functional materials. This approach may provide certain advantages from a cost savings point of view; however, any subsequent processing step is limited in terms of processing temperature. Class 1 methods are often challenged when it comes to the performance of the devices and the complexity of the circuits or systems they can produce. While new materials[9,10] including nanomaterials are sought to be the solution, many of the challenges due to the low-temperature processing requirements remain. For example, the field of printable electronics that applies electronic inks in the form of nanoparticles using direct-write inkjet-like printing methods has not yet achieved the breakthroughs since the high-temperature processing and annealing steps required from a device point of view cannot be carried out.[11–13] Class 2 – "polymeric substrate last" refers to methods that delay the use of the low-temperature substrate as long as possible. This class of methods shares the advantage that they can be combined with well-established semiconductor device technologies; the use of nanomaterials is not required. While this may look as a capitulation going back to the old and established method, it has been proven to be a very successful methodology. A pioneer in the field has been Menard et al.[14] Today, established semiconductor device technologies and segmentation (etching) methods are frequently used to produce microscopic functional device segments, which are subsequently transferred onto low-temperature substrates. Various forms of stretchable semiconductor device layers and stretchable metallic interconnects have been reported. The first examples were based on semiconductor materials such as GaAs,[2,15] InGaN,[16] and Si[15,17,18] which can be stretched and compressed (demonstrated 50%) if the thin film is transferred onto a polymeric substrate in a way to yield buckled 3D wave-like topologies[19] similar to an accordion fold. The required fabrication of very thin device layers is perhaps a slight disadvantage.

However, it is also possible to use more rigid device elements. Here, segmented devices are distributed on rubber-like substrate and electrically connected using stretchable meander shaped metallic interconnects. This approach has been particularly successful and various new applications were demonstrated; conformable optoelectronic modules,[20–22] stretchable sensor arrays,[7] and rubber-like electrocardiographic electrode arrays[23] are some examples. In contrast with the first method, this methodology enables, in principle, direct use of commercial devices and circuit elements.

As mentioned, Class 2 methods require the assembly of the device layer or the application of interconnects toward the end of the processing sequence that can be challenging as well. Finalization of the functional system requires steps of assembly, alignment, transfer, contact pad registration, or electrical contact formation that are all challenging points. For example, it is difficult to form electrical interconnects between individual layers in subsequent transfer steps. As a result, most of the reported structures complete the electrical interconnects directly on the wafer to eliminate this step. In other words, transfer of the entire structure in a single step is often used. Moreover, the stretchable systems reported so far used semiconductor device elements that had all contacts on a single face to eliminate the realization of multilayer alignment; the arrangement presented here will use devices with top and

S.-C. Park, J. Fang
Electrical and Computer Engineering
University of Minnesota
200 Union St. SE, Minneapolis, MN 55455, USA
S. Biswas, M. Mozafari, Dr. T. Stauden,
Prof. H. O. Jacobs
Fachgebiet Nanotechnologie
Technische Universität Ilmenau
Gustav-Kirchhoff-Strasse 1, D-98693 Ilmenau, Germany
E-mail: heiko.jacobs@tu-ilmenau.de

DOI: 10.1002/adma.201500839

bottom contacts that are particularly challenging from an interconnection point of view; a lamination step will be discussed to overcome this challenge. Another challenge involves limitations in the size of the stretchable systems that are currently limited to the size and layout of the donor wafer. Large-area integration and redistribution of the active devices is commonly not possible; transfer techniques use a donor substrate/wafer and maintain orientation and integration density.

This publication addresses this issue of assembly and redistribution. In the presented case, we will use conventional binned dies on a carrier tape with a pitch and orientation specified by the manufacturer, which is different from the desired final arrangement. In other words, redistribution is required and simple transfer is not possible. A process of directed self-assembly is used to achieve redistribution, alignment, and registration. The process extends the range of applications to the utilization of commercially available segmented semiconductor chips instead of previously used specially designed donor wafers to transfer the parts. As a demonstrator, we choose to fabricate a millimeter thin rubber-like solid-state-lighting module incorporating distributed and electrically connected LEDs. Fabrication of this structure incorporates: i) design and fabrication of the bottom electrode, ii) assembly and electrical connection of the LEDs, and iii) lamination of a conductive top layer. The bottom electrode is designed using a computation tool for realizing "stretch-tolerant," a "gradient," and "no-stretch-regions." The composite structure can be stretched to 220% of the original length, while the assembly sites for the chips remain within a "no-stretch-region" that is more robust than other designs. The assembly of the chips is achieved using a roll-to-roll fluidic self-assembly platform[24] that is adapted to work with the soft and rubber-like material. To complete the electrical connections and to eliminate critical alignments, a hybrid top conductive lamination layer will be presented. The laminate is composed of a conductive wire mesh (less adhesive) that is embedded in an adhesive (not conductive) matrix. The composite can tailor the electrical and adhesive properties independently and defect-free lighting modules can be formed. The origin of defects in the 1 mm thick structure under stress will be discussed.

Figure 1 provides an overview of the experimental strategy to fabricate mechanically flexible and foldable area lighting modules on the basis of solder-directed fluidic self-assembly and lamination. Our goal was to establish a scalable process to fabricate such modules in a continuous roll-to-roll process. Moreover, the process is designed to be compatible with unpackaged commercially available LED chips. We used n-GaN/p-GaN thin LEDs with a side length of 300 µm and a height of 115 µm (XT290, Cree) as device segments in this study. The fabrication of the specific area lighting module requires the use of stretchable materials and interconnects to relieve the stress as the structure is bent. Overall, the process is divided by the three required milestones to fabricate a functional unit. First, a sufficiently reliable bottom electrode with receptors that provides sufficient stretchability to relieve the stress has to be fabricated. Second, the attachment of the LEDs needs to be done over wide area substrates, which is accomplished using a solder-directed fluidic self-assembly[24–27] instead of conventional robotic pick and place or wafer level transfer. Third, the electrical connections need to be completed to operate the LED array. The third

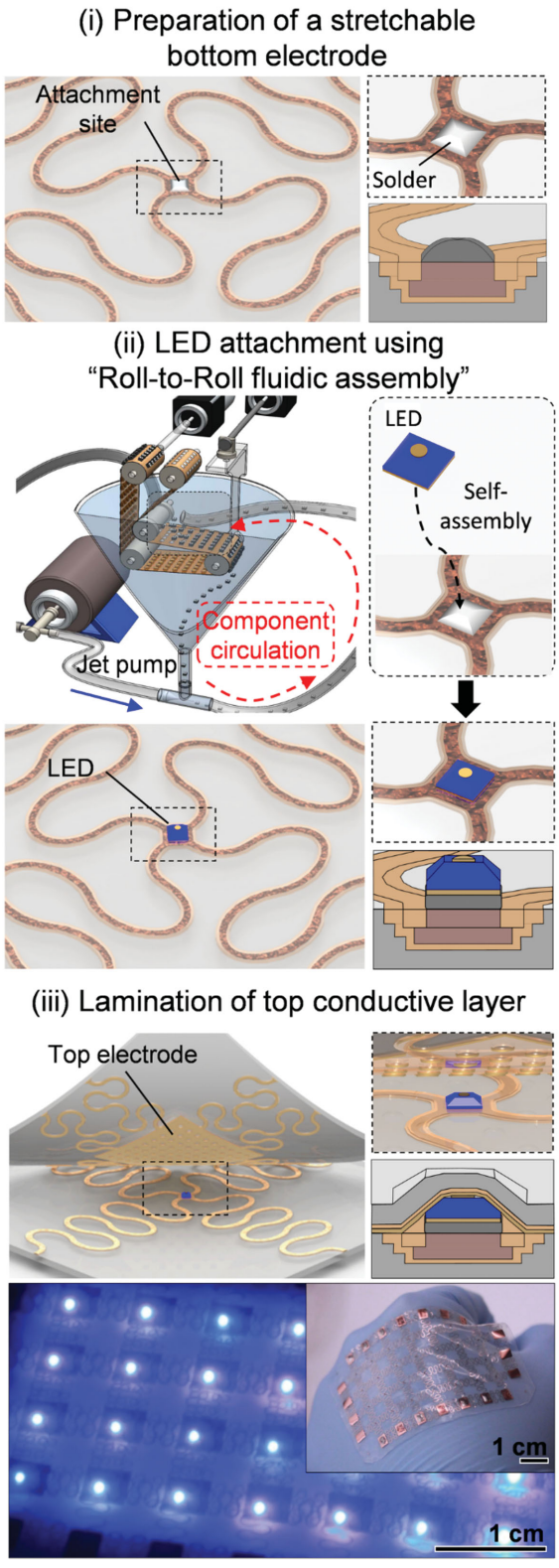

Figure 1. Overview of the three basic steps used to fabricate a rubber-like solid-state lighting module: i) preparation of a stretchable bottom electrode with solder-coated attachment site, ii) the attachment of the LEDs using solder-directed fluidic self-assembly, and iii) the lamination of a stretchable top conductive layer.

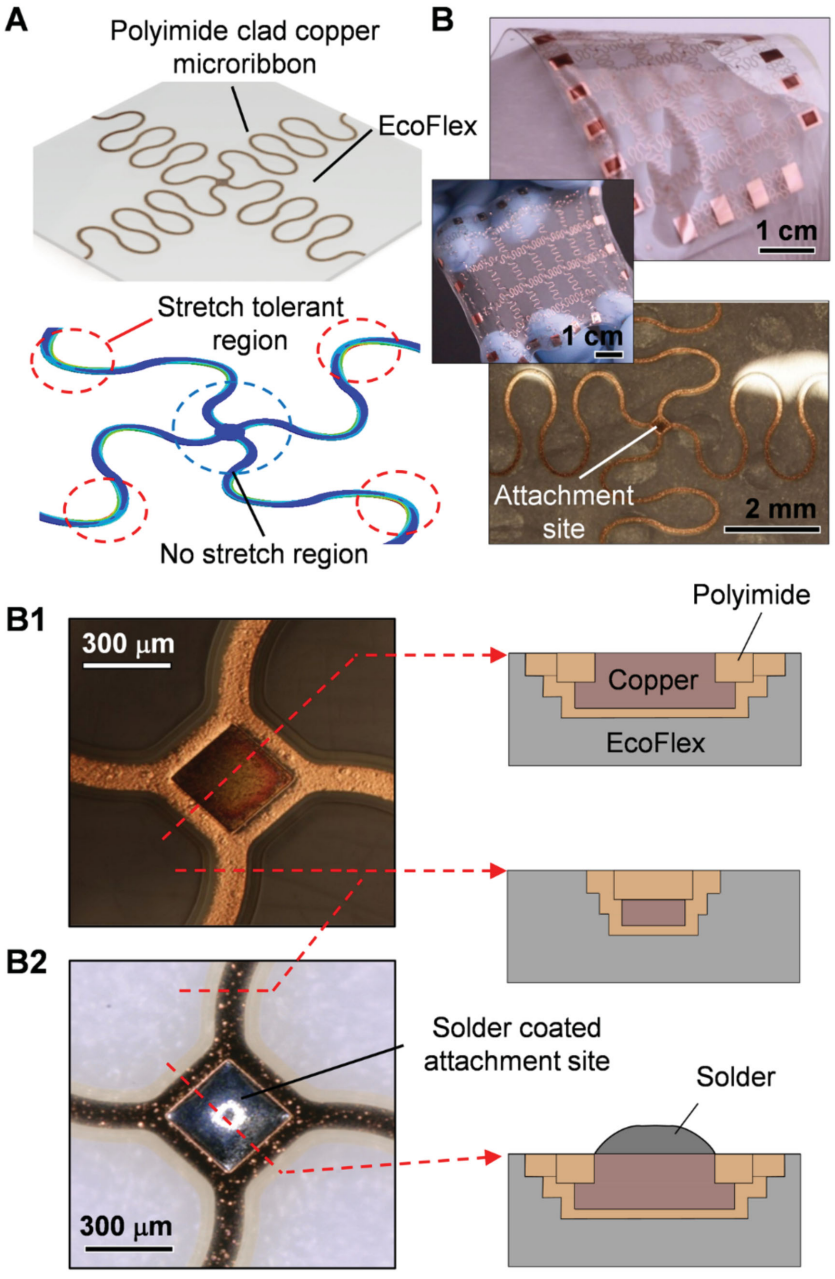

Figure 2. Schematics (A) and photographs (B) of the fabricated stretchable bottom electrode. The structure is designed to be compatible with a fluidic self-assembly process that requires the integration of a solder bump in a no-stretch-assembly region. One stress profile calculation (also being discussed in Figure 3) is shown. The profile depicts a no-stretch-region (blue circle). The no-stretch-region is the preferred location to define an attachment site for the LEDs with minimal mechanical stress. The attachment sites within the array are electrically connected using 100 μm wide and 5 μm thick meander shaped copper traces. These traces are mechanically and chemically stabilized using a polyimide cladding with the illustrated cross-sections. The color difference in the corresponding top view photographs is due to a difference in the background; a white paper cloth versus a transparent background.

step was particularly challenging; the use of wire-bonding had to be eliminated and it was required to develop a lamination step that applies a stretchable top conductive layer to the structure to complete the electrical connections (photograph, Figure 1, bottom) without any critical alignment. The required fabrication steps, technology, and present limitations will be described in the following sections.

Preparation and Characterization of the Stretchable Stress-Relieving Rubber Supported Metal Electrode: The rubber-like bottom electrode has to satisfy a number of requirements: i) it needs to be compatible with the fluidic self-assembly process we presently use; specifically, solder-based receptors and LED attachment points have to be formed which are mechanically stable during the self-assembly process and during operation, ii) the substrate needs to provide a common electrical connection to the anode of the LEDs, iii) the interconnection has to be chemically stable during the self-assembly and electrically isolated from the top conductive layer, and iv) it needs to provide a sufficient amount of mechanical stretchability to relieve the stress between the top and bottom contacts of the LEDs during folding.

While a number of previously published methods were tested,[7,22,23] we ended up with a new design as shown in **Figure 2**. Two major difficulties were found and eliminated.

The first challenge dealt with the interface between the hard and no-stretchable semiconductor dies and the soft and stretchable meander-shaped conducting matrix used as interconnection (Figure 2A). Electrical failure at the interface between hard and soft materials through crack and fracture of the metal was found to be an issue in several designs. The current design minimizes this problem and was based on computation model (Ansys Mechanical) testing several layouts with the goal to achieve a "no-stretch-region" (highlighted with the blue circle) that is larger than the LED chip. Additional calculations and a comparison of various elliptic-arc-interconnect designs are presented in Figure S1 in the Supporting Information. The chosen design was based on a compromise between redundancy in the number of parallel interconnects and required level of stretchability, which is further discussed in the Supporting Information. In brief, the depicted design minimizes mechanical stress in close proximity to the chip and diverts the stress to "stretch-tolerant-regions" (highlighted with the red circle).

The second challenge dealt with the realization of a stretchable interconnect region that is compatible with the fluidic self-assembly process. Previous research used a stretchable interconnect that was tailored to work with conventional robotic assembly.[21,22] These were not sufficiently stable in our experiments. Several modifications were required to support the fluidic self-assembly process. A complete surrounding of the metallic conductor with a polyimide cladding

was required to achieve the mechanical and chemical stability necessary to support subsequent processes such as solder dip-coating and fluidic self-assembly. Without such a cladding, the metal was insufficiently stable during the solder wetting process. Delamination and fracture occurred during the solder dip-coating process. Even in regions that did survive the solder dip-coating process the metal meander was not sufficiently stable when being stretched. Both problems were eliminated introducing the "polyimide-clad-copper-microribbons", which are traces of copper that are completely surrounded with upper and lower polyimide cladding. The cladding provides additional mechanical strength and additional adhesion to the EcoFlex substrate. Moreover, the polyimide cladding provides an effective method to prevent solder wetting in the stretchable interconnect regions. At the same time, it can be lithographically patterned and a window can be defined to access the copper. The ability to define windows is also essential from a self-assembly point of view; the fabrication of non-stretchable chip attachment points and subsequent chip attachment on the basis of solder wetting requires these windows. From a fabrication point of view, the "polyimide-clad-copper-microribbons" are supported on top of a silicone rubber (EcoFlex, Smooth-On) based substrate; Figure S2 (Supporting Information) details the fabrication steps. Attachment sites for the self-assembly are formed using square-shaped windows in the upper polyimide cladding to access the copper that is subsequently coated with solder (Indalloy #117, MP. 47 °C, Indium Corp., NY) through dip-coating. LED attach at these locations using the self-assembly process discussed later.

From a stretchability point of view, the bottom electrode can be stretched to about 220% (elongated by a factor of 2.2) before electrical failure occurs. Careful analysis, however, shows that the ribbons begin to delaminate from the EcoFlex substrate when being stretched to about 170% of the original length. In the range from 170% to 200% flexing and torsion becomes clearly visible that agree well with computational analysis of these types of unsupported metal ribbons (**Figure 3**A–C). The torsion is a result of the buildup of strain and stress at the outer and inner edges of the meander. We would like to note that the stress-relieving mechanism through torsion and delamination is not possible in any device where the metal is sandwiched in between two slabs of EcoFlex. This leads to higher strain on metal traces that eventually cause an earlier failure. For example, as soon as a meander is fully encapsulated with EcoFlex the electrical connections begin to fail at an approximate stretch of 170% of the original length using the current design (5 μm thick and 100 μm wide copper ribbon surrounded with a 8 μm top and 7 μm bottom polyimide cladding (150 and 200 μm wide, respectively). This stretch limit can likely be increased through a reduction of the widths of the ribbons.

All the stretching experiments involved anchoring one end of the fabricated electrode to a fixed support, while the other end is attached to freely moving support. As a result, the reported numbers are for the condition of uniaxial stretching in both the x and y directions. The previously mentioned 170% represents the limit before irreversible interfacial delamination occurs. The rupture and electrical discontinuity depicted in Figure 3D occurred at around 220% stretch along the x direction. The encapsulation with a second slap of EcoFlex brings

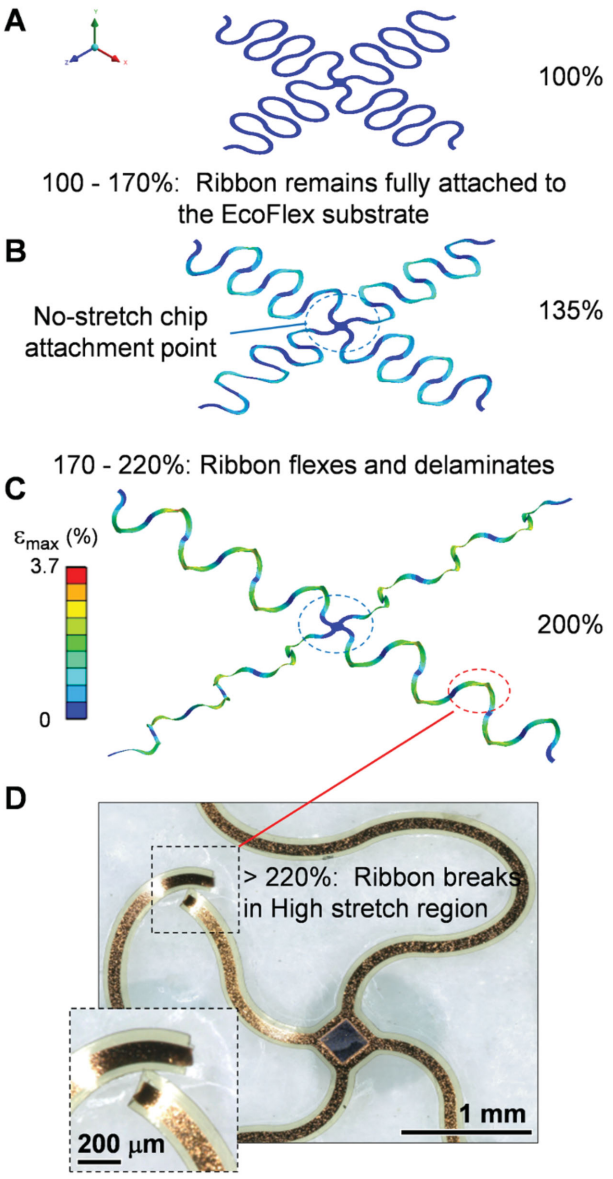

Figure 3. Computational analysis and photograph depicting strain (color coded) and mechanical torsion and flexing (Ansys) of the metal ribbons. A) Reference structure, not being stretched. B) Reversible stretch region (100–170%); ribbons remain mainly attached to the EcoFlex substrate. C) Irreversible stretch region (170–220%) leading to complete delamination; localized flexing and torsion of the ribbon is visible. D) Typical failure exceeding the 220% stretch limit.

up the question whether voids and air bubbles are introduced as the structure is stretched. The introduction of voids would require a vertical separating force. Indeed, there is an origin of a vertical force that is the torsion of the ribbon (clearly visible in Figure 3C). However, in our design, the torsion was not sufficiently strong to cause the formation of stress relieving voids; the ribbon would rupture first.

We have also measured the electrical resistance of the bottom and top electrodes as it is being stretched (Supporting information, Figure S3A,B). On the bottom electrode, the electrical resistance remains constant up to 220% stretch. Afterward,

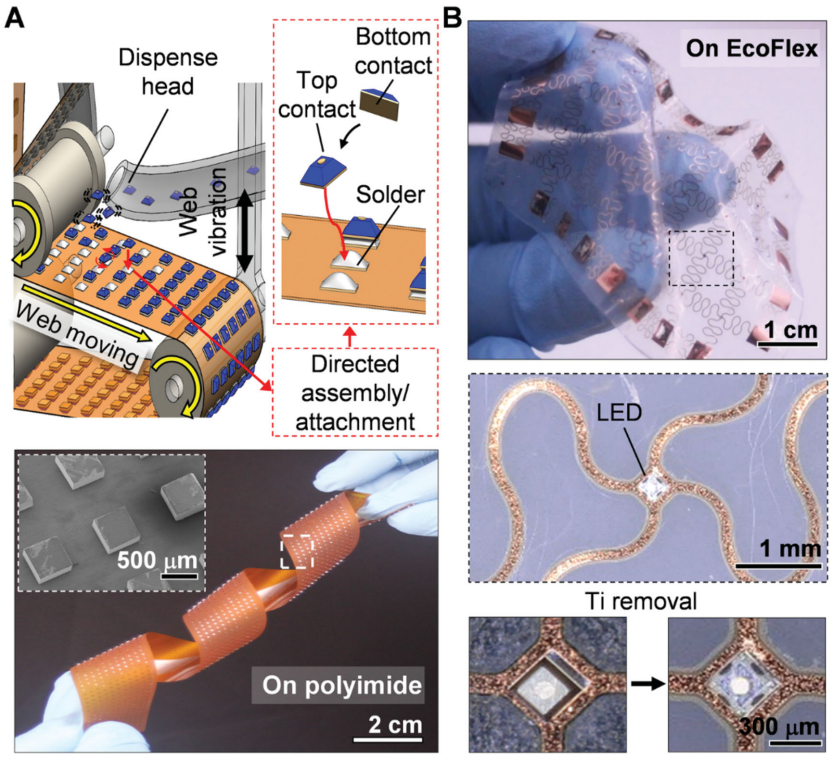

Figure 4. Chip attachment using roll-to-roll fluidic assembly and photographs of the resulting structures. A) The application and assembly of the chips is achieved using localized application using a dispensing head and directed assembly using surface tension-driven assembly.[24] The molten solder bumps have a high surface energy that leads to the attachment and alignment of the chips and the formation of an electrical contact to the anode of chips. Results of assembled chips with a high density (bottom left) and a low area density (right) are shown. A 100 nm thick Ti layer is used as an anti-solder wetting layer to ensure correct right-side-up (negative terminal facing up) LED assembly; this Ti layer is removed in 45 s Ti etch (B, bottom) prior to the lamination of the stretchable top contact.

we observe an increase in the resistance due to an irreversible mechanical fracture in the stretch tolerant region. The fracture occurs at the predicted location based on the mechanical stress profile calculations (Figure 3C,D). The top electrode has a different layout. It uses a reduced meander length. As anticipated, the onset of the irreversible mechanical failure occurs earlier with a reduction of the meander length. The electrical resistance remains constant up to 130% stretch.

Attachment of the LEDs using Solder-Directed Fluidic Self-Assembly: We assembled the LEDs on the solder-coated attachment sites utilizing a roll-to-roll fluidic self-assemble machine that has been reported recently.[24] It applies LEDs to desired areas on a continuously advancing web using a nozzle, which is similar to conventional printing of inks. However, localized electrical attachment is based on directed self-assembly on the basis of surface tension-driven assembly involving a conductive adhesive or solder.[24–29] The reported process (**Figure 4**) is able to assemble semiconductor chips onto continuously advancing substrates with a yield approaching 100%. We used 9000 LED chips in the roll-to-roll fluidic assembly platform. The chips circulate through the system. Access chips are captured at the bottom and reintroduced at the assemble sites. Several adaptations had to be made to get defect-free assemblies using the EcoFlex rubber-like substrates used in this study. EcoFlex caused problems due to non-specific adhesion that hinders the movement and distribution of the components on the substrate. To minimize this non-specific adhesion, a combination of an oxygen plasma treatment (3 min, 100 W, 100 sccm O_2) of EcoFlex surface and the use of a non-ionic surfactant inside the assembly solution (Triton X-100, Sigma–Aldrich, 5 mL per 1 L assembly solution) was required. Freely moving components on the substrate were only observed after this treatment. As a result, it was possible to achieve defect-free assemblies on the EcoFlex substrates as illustrated in Figure 4B.

It is also important to point out that the LED has two contacts, a small circular top contact and a large square bottom contact. Correct assembly is only possible if the top sides are modified to ensure that the chips assemble with the correct (bottom side) contact on the substrate. This requires the application of a sacrificial 100 nm thick and sputter-coated Ti anti-solder wetting layer onto the top face of the LEDs prior to the self-assembly. Solder does not wet this Ti layer that ensures that the chips assemble with the correct orientation on the substrate (Figure 4B, bottom, left). The Ti coating of correctly assembled LEDs is removed using a 45 s long wet chemical etch (Figure 4B, bottom, right).

After LED assembly we tested the stretchability of the array. The structure maintained the electrical conductivity up to the previously established 220% stretch limit. Most importantly, the introduced localized "no-stretch" assembly sites were found to be very effective to minimize strain; no detachment of the LEDs at these sites was observed during the stretch experiments that means that the meander-shaped interconnects would fail first. This is a dramatic improvement over earlier designs where we lost most of the chips as a result of delamination when the substrate was stretched. Moreover, the design satisfied the required mechanical and chemical stability for the self-assembly process. For example, no mechanical damage to the bottom electrode was observed as a result of the assembly process.

Preparation and Characterization of a Stretchable Conductive Top Layer, Lamination, and Testing of the Final Device: The completion of the lighting module requires the realization and lamination of the top electrode (**Figure 5**). Our goal was to eliminate conventional serial wire-bonding that is commonly used to contact the top layer of the LEDs and to replace this step using a method that can, in principle, be scaled to a roll-to-roll processing scheme. A solution to this problem is critical since it could lower the production cost and enable processing over larger areas. An ideal method would be a simple lamination step.

To accomplish these goals, the top laminate needs to be conductive, provide some level of adhesion, and form electrical interconnects to the top contact of the LEDs. Moreover, the

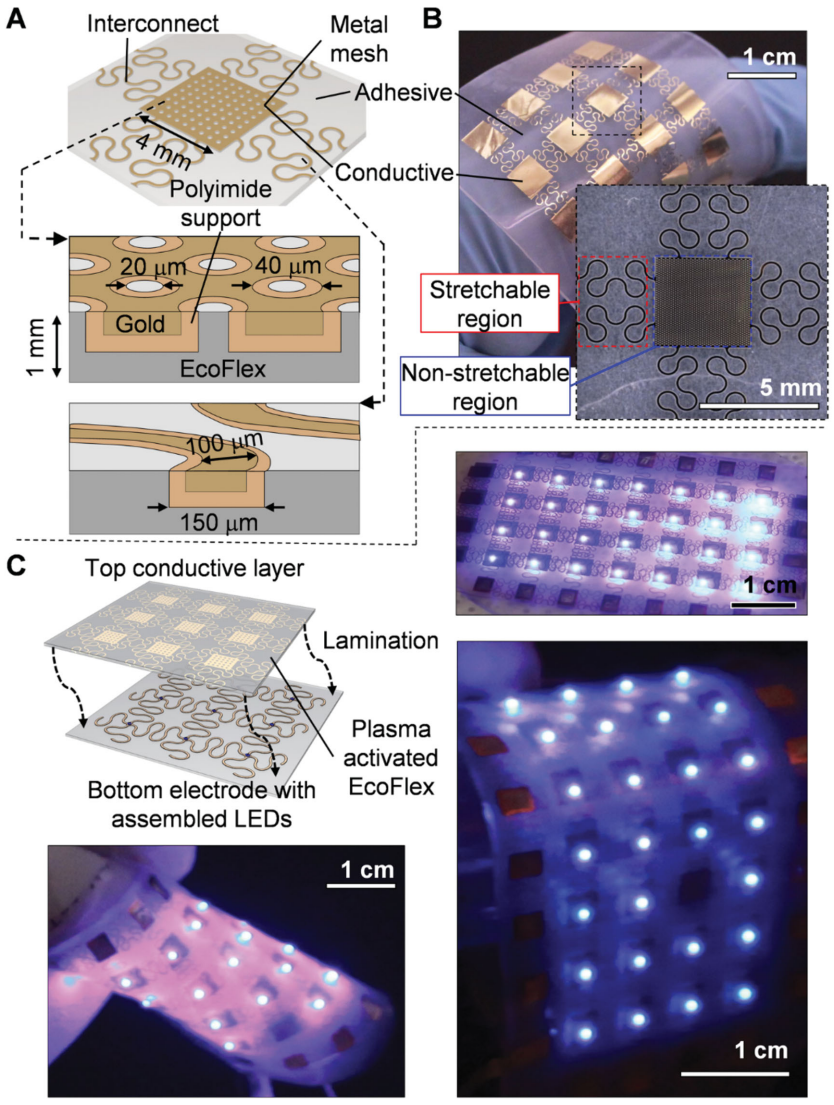

Figure 5. Schematics and photographs describing the design, fabrication, and application of the stretchable top conductive lamination layer next to results of a completed 2 mm thin rubber-like module under test. A) The designed laminate is a composite made up of: i) conductive and ii) adhesive as well as iii) stretchable (meander), and iv) non-stretchable (metal mesh) regions; oxygen plasma activated EcoFlex acts as an adhesive during the lamination process. The 20 μm in diameter intermediate EcoFlex bonding sites hold the metal mesh in place which in turn contacts the top contact of the LEDs. A weak point of the current design is the abrupt transition from the "non-stretchable" mesh to the "stretchable" meander. Here, the polyimide support (a partial cladding visible in (A)) improves the mechanical stability. B) Photographs of the realized stretchable top conductive laminate. C) The lamination is presently done by hand; as a consequence, we used a 4 mm × 4 mm metal mesh to tolerate a 2 mm misalignment with respect to the center contact of the LED. Outside this limit, the top contact will not be contacted. The bottom photograph shows a completed lighting module under various levels of deformation.

laminate needs to relieve mechanical stress when the structure is bent. Figure 5A,B shows the design next to the fabrication result; Figure S4 (Supporting Information) provided a flowchart of the fabrication steps. We introduce a laminate that integrates three design elements.

First, the laminate uses a composite materials approach whereby portions of the surface are more adhesive (not conductive) and other portions are conductive (less adhesive), which allows us to tailor the adhesive strength and interconnect resistance over a wider range then otherwise possible. The adhesive, here in the form of oxygen plasma-activated silicone rubber, is used to hold the metal–polyimide support structures in place. The approach provides a contact force that pushes the slightly protruding conducting metal (Au or Cu) in contact with the LEDs.

Second, the laminate features an anisotropic stretchable profile that is composed of no-stretch domains (locations to host the rigid and hard LED chips) and high-stretch domains (locations of the stretchable interconnects between isolated device segments), which is more robust when compared with laminates with an isotropic stretch profile.

Third, the laminate eliminates the requirement of critical alignment through the use of a tight metal mesh that provides redundant pathways to the top contacts on the chips. In other words, the gold mesh is designed to be very fine using a pitch (40 μm) that is smaller than the diameter (100 μm) of the top contact. The combination of high-pitch mesh that is extended over larger areas (4 mm × 4 mm) has several benefits: i) it eliminates critical alignment steps so that alignment can be done by hand, ii) it provides a number of redundant electrical pathways and electrical connection points (a 2 × 2 redundancy in the current design) to the top contact of the LEDs, and iii) it provides room to expose the intermediate adhesive material (EcoFlex) that increases the mechanical adhesion of this interface. The pitch of LED attachment site (7 mm) was chosen by considering several factors such as distribution of light, aspects to aid in fabrication, and overall desired size of the substrate. The most important factor to aid in the fabrication was the size of the straight-wire-metal-mesh that connects to the top contact of the LEDs. We use 2.5 turns interconnects with a 0.45 mm amplitude for the top conductive layer.

Figure 5C provides images of a functional laminate containing 28 LEDs. Several images of the structure are shown as the structure is bent into different shapes. The entire thickness of the structure is 2 mm. So far, we have tested several structures and typically we observe discontinuities in the electrical connection to appear somewhere in the array when the structure is bent to an approximate 1 cm radius of curvature resulting in a defect as shown. We were expecting to achieve a smaller (about 0.5 cm) radius of curvature since the compressive and tensile stress should be in the 10–20% range; the actual numbers depend on the location of the neutral plane; assuming a location close to the center of the slab, it is equal to the

thickness/(2 × radius of curvature), which is 10%; assuming that the location of the neutral plane is shifted toward one side of the slab it would become 20%. Independent of this detail, the top and bottom electrodes alone provided a higher level of stretchability than the calculated 20% upper limit that means that the illustrated defects cannot be a result of fracture of the meander-shaped interconnects. Instead, the cause is an insufficient adhesion between the cathode of LEDs and the top conductive layer leading to interfacial delamination that is a reversible defect. This means that it is possible to apply weak pressure to repair this interface to light up the disconnected LED. Moreover, the structure can be stretched up to 120% of the original length. Beyond this point, LEDs in the array begin to turn dark again as a result of interfacial delamination between the metal grid and the top contact; again, a full recovery of the function is possible using the application of pressure. The first permanent failure mode is reached when the structure is stretched to about 135%; at this point, we were able to record fracture of the meander shaped interconnect in the high stress region; the relatively large metal mesh region, the bottom electrode, and bottom contacts to the LEDs remained intact. To summarize, the weak point of the assembled structure is currently the top layer and, in particular, the contact to the cathode. We anticipate further improvements using designs that increase the adhesion at this interface.

Inorganic LEDs are essentially hard objects and area lighting panels with distributed LEDs are often sought of being planar and mechanically rigid. However, in principle, it is possible to design rubber-like and mechanically soft lighting structures using inorganic semiconductors if we learn how to distribute and electrically connect microscopic LED chips in a rubber-like matrix. The presented structure was a first step in this direction. The focus of this report was an intentionally chosen multilayer sandwich structure that is more challenging to fabricate when compared to previously reported structures where the device contacts are on a single face.[16,20,22,30] As a result, more steps are required: i) design of the stretchable bottom electrode, ii) assembly and electrical connection of microscopic LEDs using a roll-to-roll fluidic self-assembly step, and iii) the lamination of the top electrode that is different from prior designs. The following key elements have been learned. The combination of "stretch-tolerant" regions with "no-stretch attachment sites" reduced the bond failure to the chips; the bonds remain intact and sustain the 220% stretch limit set by the meander-shaped interconnects. The introduced polyimide cladding increased the robustness of the meander and helped to achieve this number. Such high numbers have been reported previously using meander-shaped conductors facing an air interface;[31] however, we would like to point out that out-of-plane torsion leads to delamination and controlled pop-up of the conductors under these conditions; this behavior is known to close observers of the field.[22,32,33] With the lamination of the top electrode a sandwich structure forms and the relief of this stress through out-of-plane torsion and pop-up of interconnects is no longer possible. As a result, the extremely high level of stretchability will be lost in applications that require encapsulation. This is interesting; most practical applications will require protection and some kind of encapsulation.[20,21,32,34]

The achieved flexibility and radius of curvature of the entire sandwich structures was not as good as anticipated. The reason appears to be an insufficient force and bond to form a reliable electrical contact between the top of the LEDs and the top laminate. However, the approach to form this contact is new; it was based on hybrid materials approach using a metal grid with openings to an adhesive to attach the structure. Optimization of this interface has not been done and would require adjustments to the feature size and area of the non-conductive adhesive versus feature size and area of metallic surface.

The use of fluidic self-assembly on stretchable and rubber-like substrates, on the other hand, was very successful since the assembly yield and speed is on par or better than robotic methods. The process supports the assembly of smaller chips, assembly on nonplanar and soft substrates, and higher volume when compared with conventional serial robotic pick and place and wire-bonding.

Finally, the presented methods are not limited to the realization of solid-state lighting panels. It could be extended to other applications in the fields of wearable electronics, energy harvesting, conformable photovoltaics, and electronic or biomedical skins. Applications that require the realization of multicomponent systems and not just the repetition of a single chip type would certainly be more challenging. However, in principle, such systems could be made. It would require the use of concepts such as shape recognition to enable flip-chip self-assembly with unique angular alignment or methods of sequential self-assembly to assemble more than one component/chip type on the surface.

Experimental Section

Bottom Electrode: 500 μm thick Si wafers (University Wafers, Boston, MA, USA) were first cleaned in a solution of H_2SO_4 + H_2O_2 for 15 min and rinsed with DI water. Following the cleaning step, poly(methyl methacrylate) (PMMA) was used as a releasing layer. Specifically, 950 PMMA C4 (MicroChem) was spin-coated onto the substrate at 2000 rpm for 30 s. After baking at 180 °C for 3 min, a polyimide sacrificial layer (PI2610, HD Microsystem) was spin-coated onto the substrate at 3000 rpm for 30 s and prebaked at 100 °C for 3 min. The polyimide layer was then fully cured in convection oven at 200 °C for 5 h. The primary photoimageable polyimide layer (HD4100, HD Microsystem) was spin-coated at 2000 rpm for 30 s followed by prebaking at 90 °C for 100 s and 100 °C for 100 s subsequently. The substrate was then exposed with 192 mJ cm^{-2} UV light, developed in PA 401D (HD Microsystem) for 150 s and rinsed in PA 400R (HD Microsystem) for 10 s. After drying, 10 nm Ti and 200 nm Cu were sputter deposited onto the substrate. Photoresist (AZ9260, AZ Electronic Materials) was then applied at 2000 rpm, prebaked at 110 °C for 165 s, and exposed with 500 mJ cm^{-2} UV light. The photoresist was developed using a 1:4 solution of AZ 400K developer diluted with DI water for 3 min. Subsequently, a thick copper layer was electroplated in 2:5:20 solution of $CuSO_4$ + H_2SO_4 + DI water for 15 min. The photoresist was removed using a reactive ion etching (RIE) process (O_2, 100 sccm, 100 W, 100 mTorr). The thin sputtered Cu and Ti layers were subsequently wet-etched in 30% $FeCl_3$ and buffered oxide etch solutions. The fabrication of secondary polyimide layer followed the same process with the primary polyimide layer above. After patterning the secondary polyimide layer, a silicone rubber precursor (EcoFlex 00-30, Smooth-On, Inc.) was poured onto the substrate and cured at room temperature for 4 h. The entire bottom electrode was then transferred to silicone rubber from the Si substrate by removing PMMA releasing layer with acetone. The remaining polyimide sacrificial layer was removed using RIE (80 sccm O_2 + 20 sccm CF_4, 200 W, 100 mTorr). Finally, the receptor was formed by dip-coating in a heated solder bath.

Top Conductive Layer: The fabrication of the top conductive lamination layer followed the cleaning process, coating PMMA releasing layer, and polyimide sacrificial layer process above. After coating the sacrificial layer, 10 nm Cr and 250 nm Au were deposited using an e-beam evaporator onto the substrate. Photoresist (Microposit 1813 Shipley) was applied (3000 rpm), exposed, and developed in 1 Microposit 351:5 H_2O developer (25 s). The Au and Cr layers were subsequently wet-etched followed by removing the photoresist using RIE. Subsequent processes such as patterning the polyimide layer, applying the silicone rubber support, transfer, release, removal of the sacrificial layer were identical to what had been described above. Before lamination step the silicone rubber surface was activate using O_2 plasma (100 sccm, 100 W, 100 mTorr).

Supporting Information

Supporting Information is available from the Wiley Online Library or from the author.

Acknowledgements

The research received financial support in part through grants from the National Science Foundation (NSF Grant DMI-1068013), German Science Foundation (DFG Grants JA 1023/3-1), and the Carl-Zeiss Foundation.

Received: February 16, 2015
Revised: April 9, 2015
Published online: May 12, 2015

[1] W. Zeng, L. Shu, Q. Li, S. Chen, F. Wang, X.-M. Tao, *Adv. Mater.* **2014**, *26*, 5310.
[2] J. Lee, J. Wu, M. Shi, J. Yoon, S.-I. Park, M. Li, Z. Liu, Y. Huang, J. A. Rogers, *Adv. Mater.* **2011**, *23*, 986.
[3] A. M. Gaikwad, A. M. Zamarayeva, J. Rousseau, H. Chu, I. Derin, D. A. Steingart, *Adv. Mater.* **2012**, *24*, 5071.
[4] M. Kaltenbrunner, G. Kettlgruber, C. Siket, R. Schwödiauer, S. Bauer, *Adv. Mater.* **2010**, *22*, 2065.
[5] T. Someya, Y. Kato, T. Sekitani, S. Iba, Y. Noguchi, Y. Murase, H. Kawaguchi, T. Sakurai, *Proc. Natl. Acad. Sci. USA* **2005**, *102*, 12321.
[6] B. C.-K. Tee, C. Wang, R. Allen, Z. Bao, *Nat. Nanotechnol.* **2012**, *7*, 825.
[7] D.-H. Kim, N. Lu, R. Ma, Y.-S. Kim, R.-H. Kim, S. Wang, J. Wu, S. M. Won, H. Tao, A. Islam, K. J. Yu, T.-i. Kim, R. Chowdhury, M. Ying, L. Xu, M. Li, H.-J. Chung, H. Keum, M. McCormick, P. Liu, Y.-W. Zhang, F. G. Omenetto, Y. Huang, T. Coleman, J. A. Rogers, *Science* **2011**, *333*, 838.
[8] R. C. Webb, A. P. Bonifas, A. Behnaz, Y. Zhang, K. J. Yu, H. Cheng, M. Shi, Z. Bian, Z. Liu, Y.-S. Kim, W.-H. Yeo, J. S. Park, J. Song, Y. Li, Y. Huang, A. M. Gorbach, J. A. Rogers, *Nat. Mater.* **2013**, *12*, 938.
[9] T. Sekitani, H. Nakajima, H. Maeda, T. Fukushima, T. Aida, K. Hata, T. Someya, *Nat. Mater.* **2009**, *8*, 494.
[10] L. Hu, M. Pasta, F. L. Mantia, L. F. Cui, S. Jeong, H. D. Deshazer, J. W. Choi, S. M. Han, Y. Cui, *Nano Lett.* **2010**, *10*, 708.
[11] K.-Y. Chun, Y. Oh, J. Rho, J.-H. Ahn, Y.-J. Kim, H. R. Choi, S. Baik, *Nat. Nanotechnol.* **2010**, *5*, 853.
[12] A. P. Robinson, I. Minev, I. M. Graz, S. Lacour, *Langmuir* **2011**, *27*, 4279.
[13] B. Y. Ahn, E. B. Duoss, M. J. Motala, X. Guo, S.-I. Park, Y. Xiong, J. Yoon, R. G. Nuzzo, J. A. Rogers, J. A. Lewis, *Science* **2009**, *323*, 1590.
[14] E. Menard, K. J. Lee, D.-Y. Khang, R. G. Nuzzo, J. A. Rogers, *Appl. Phys. Lett.* **2004**, *84*, 5398.
[15] Y. Sun, W. M. Choi, H. Jiang, Y. Y. Huang, J. A. Rogers, *Nat. Nanotechnol.* **2006**, *1*, 201.
[16] S.-I. Park, Y. Xiong, R.-H. Kim, P. Elvikis, M. Meitl, D.-H. Kim, J. Wu, J. Yoon, C.-J. Yu, Z. Liu, Y. Huang, K.-c. Hwang, P. Ferreira, X. Li, K. Choquette, J. A. Rogers, *Science* **2009**, *325*, 977.
[17] D.-Y. Khang, H. Jiang, Y. Huang, J. A. Rogers, *Science* **2006**, *311*, 208.
[18] D.-H. Kim, J.-H. Ahn, W. M. Choi, H.-S. Kim, T.-H. Kim, J. Song, Y. Y. Huang, Z. Liu, C. Lu, J. A. Rogers, *Science* **2008**, *320*, 507.
[19] C. M. Stafford, C. Harrison, K. L. Beers, A. Karim, E. J. Amis, M. R. Vanlandingham, H.-C. Kim, W. Volksen, R. D. Miller, E. E. Simonyi, *Nat. Mater.* **2004**, *3*, 545.
[20] R.-H. Kim, D.-H. Kim, J. Xiao, B. H. Kim, S.-I. Park, B. Panilaitis, R. Ghaffari, J. Yao, M. Li, Z. Liu, V. Malyarchuk, D. G. Kim, A.-P. Le, R. G. Nuzzo, D. L. Kaplan, F. G. Omenetto, Y. Huang, Z. Kang, J. A. Rogers, *Nat. Mater.* **2010**, *9*, 929.
[21] D. Ruh, P. Reith, S. Sherman, M. Theodor, J. Ruhhammer, A. Seifert, H. Zappe, *Adv. Mater.* **2014**, *26*, 1706.
[22] X. Hu, P. Krull, B. d. Graff, K. Dowling, J. A. Rogers, W. J. Arora, *Adv. Mater.* **2011**, *23*, 2933.
[23] S. Xu, Y. Zhang, L. Jia, K. E. Mathewson, K.-I. Jang, J. Kim, H. Fu, X. Huang, P. Chava, R. Wang, S. Bhole, L. Wang, Y. J. Na, Y. Guan, M. Flavin, Z. Han, Y. Huang, J. A. Rogers, *Science* **2014**, *344*, 70.
[24] S.-C. Park, J. Fang, S. Biswas, M. Mozafari, T. Stauden, H. O. Jacobs, *Adv. Mater.* **2014**, *26*, 5942.
[25] H. O. Jacobs, A. R. Tao, A. Schwartz, D. H. Gracias, G. M. Whitesides, *Science* **2002**, *296*, 323.
[26] R. J. Knuesel, H. O. Jacobs, *Proc. Natl. Acad. Sci. USA* **2010**, *107*, 993.
[27] W. Zheng, P. Buhlmann, H. O. Jacobs, *Proc. Natl. Acad. Sci. USA* **2004**, *101*, 12814.
[28] Y. Li, K.-S. Moon, C. P. Wong, *J. Electron. Mater.* **2005**, *34*, 266.
[29] U. Srinivasan, M. A. Helmbrecht, C. Rembe, R. S. Muller, R. T. Howe, *IEEE J. Sel. Top. Quantum Electron.* **2002**, *8*, 4.
[30] H.-s. Kim, E. Brueckner, J. Song, Y. Li, S. Kim, C. Lu, J. Sulkin, K. Choquette, Y. Huang, R. G. Nuzzo, J. A. Rogers, *Proc. Natl. Acad. Sci. USA* **2011**, *108*, 10072.
[31] S. Xu, Y. Zhang, J. Cho, J. Lee, X. Huang, L. Jia, J. A. Fan, Y. Su, J. Su, H. Zhang, H. Cheng, B. Lu, C. Yu, C. Chuang, T.-I. Kim, T. Song, K. Shigeta, S. Kang, C. Dagdeviren, I. Petrov, P. V. Braun, Y. Huang, U. Paik, J. A. Rogers, *Nat. Commun.* DOI: 10.1038/ncomms2553
[32] D.-H. Kim, J. Song, W. M. Choi, H.-S. Kim, R.-H. Kim, Z. Liu, Y. Huang, K.-C. Hwang, Y.-W. Zhang, J. A. Rogers, *Proc. Natl. Acad. Sci. USA* **2008**, *105*, 18675.
[33] D. S. Gray, J. Tien, C. S. Chen, *Adv. Mater.* **2004**, *16*, 393.
[34] Y. Hattori, L. Falgout, W. Lee, S.-Y. Jung, E. Poon, J. W. Lee, I. Na, A. Geisler, D. Sadhwani, Y. Zhang, Y. Su, X. Wang, Z. Liu, J. Xia, H. Cheng, R. C. Webb, A. P. Bonifas, P. Won, J.-W. Jeong, K.-I. Jang, Y. M. Song, B. Nardone, M. Nodzenski, J. A. Fan, Y. Huang, D. P. West, A. S. Paller, M. Alam, W.-H. Yeo, J. A. Rogers, *Adv. Healthcare Mater.* **2014**, *3*, 1597.